NanoThailand 2016

Estimation of density of interface state and carrier transportation mechanism of heterojunctions comprising of n-type nanocrystalline $FeSi_2$ thin films and p-type Si substrates fabricated utilizing pulsed laser deposition

Adison Nopparuchikun*, Nathaporn Promros*, Phongsaphak Sittimart, Peeradon Onsee, Asanlaya Duangrawa, and Sakmongkon Teekchaicum

Department of Physics, Faculty of Science, King Mongkut's Institute of Technology Ladkrabang, Bangkok 10520, Thailand

---

Abstract

Utilizing pulsed laser deposition (PLD), heterojunctions comprising of n-type nanocrystalline (NC) $FeSi_2$ thin films and p-type Si substrates were fabricated at room temperature in this present study. Both dark and illuminated current density-voltage (*J-V*) curves for the heterojunctions were measured and analyzed at room temperature. The heterojunctions demonstrated a large reverse leakage current as well as a weak near-infrared light response. Based on the analysis of the dark forward *J-V* curves, at the V value ≤ 0.2 V, a carrier recombination process was governed at the heterojunction interface. When the V value was > 0.2 V, the probable mechanism of carrier transportation was a space-charge limited-current process. Both the measurement and analysis for capacitance-voltage-frequency (*C-V-f*) and conductance-voltage-frequency (*G-V-f*) curves were performed in the applied frequency (f) range of 50 kHz - 2MHz at room temperature. From the *C-V-f* and *G-V-f* curves, the density of interface states (N_{ss}) for the heterojunctions was computed by using the Hill-Coleman method. The N_{ss} values were 2.38×10^{12} $cm^{-2}eV^{-1}$ at 2 MHz and 2.72×10^{13} $cm^{-2}eV^{-1}$ at 50 kHz, which proved the existence of interface states at the heterojunction interface. These interface states are the probable cause of the degraded electrical performance in the heterojunctions.

Selection and Peer-review under responsibility of 5th Thailand International Nanotechnology Conference (NanoThailand 2016)
Keywords: NC-$FeSi_2$/Si heterojunctions, *J-V* curve, *C-V-f* curve, *G-V-f* curve, interface state

---

1. Introduction

Several researchers have reported that semiconducting iron disilicide (β-$FeSi_2$) comprising of nontoxic elements (Si and Fe), has attracted much attention recently as a new promising candidate for application in silicon-based optoelectronic devices [1-4]. It is because β-$FeSi_2$ possesses both indirect and direct optical bandgaps of 0.74 eV, and 0.85 eV, respectively. These optical bandgap values are of relevance to optical fiber telecommunication wavelengths [5-7]. Additionally, β-$FeSi_2$ grown epitaxially on Si with small lattice mismatches [8-10] has an optical absorption coefficient of more than 10^5 cm^{-1} at 1.2 eV [11-13]. Nanocrystalline (NC) $FeSi_2$ grown on any solid substrate at room temperature possesses semiconducting features close to β-$FeSi_2$ [14-16]. It is comprised of a crystal with diameter range of 3-5 nm [17] and has a larger optical absorption coefficient than β-$FeSi_2$ [18-19]. Thus, NC-$FeSi_2$ is an attractive material for application in silicon-based optoelectronic devices.

In a previous study, NC-$FeSi_2$ thin films grown utilizing pulsed laser deposition (PLD) were investigated for their structural and electrical features [17]. The NC-$FeSi_2$ thin films possessed n-type conduction and a carrier density ranging between 10^{18} to 10^{19} cm^{-3}[17]. After that, the near-infrared (NIR) light detection performance for the n-type NC-$FeSi_2$/p-type Si heterojunctions fabricated utilizing PLD was studied [14]. Based on the experimental results, the fabricated heterojunctions demonstrated a large reverse leakage current and a weak NIR light response at room temperature. A probable cause was likely the existing interface states at the heterojunction interface between

* Corresponding author. Tel.: +66 2-329-8400; fax: +66 2-329-8412.
E-mail address: adisonnopparuchikun@gmail.com, nathaporn_promros@kyudai.jp

Selection and Peer-review under responsibility of 5th Thailand International Nanotechnology Conference (NanoThailand 2016)

NC-$FeSi_2$ and Si acting as a center of leakage current and a trap center for photo-generated carriers [14-16]. However, the estimations of the density of interface state (N_{ss}) and the probable transportation mechanisms of the carrier at the heterojunction interface between the NC-$FeSi_2$ and Si have not been studied in detail yet.

In the present study, the measurement and analysis of capacitance-voltage-frequency (*C*-*V*-*f*) and conductance-voltage-frequency (*G*-*V*-*f*) curves of the n-type NC-$FeSi_2$/p-type Si heterojunctions fabricated utilizing PLD were performed at room temperature. The N_{ss} value at the heterojunction interface between the NC-$FeSi_2$ and Si was computed utilizing the Hill-Coleman method. It proved the existence of interface states for the heterojunctions in this study. These interface states probably are the cause of the degraded electrical properties in the aforementioned heterojunctions. Additionally, the probable transportation mechanism of the carrier through the heterojunction interface was studied. At $V \leq 0.2$ V, the predominant transportation mechanism of the carriers was the recombination process. It was governed by a space-charge-limited current (SCLC) process at $V > 0.2$ V. Based on all the knowledge avaliable to the authors, this study is the first investigation of the N_{ss} value and probable transportation mechanisms of the carrier at room tempearture for the n-type NC-$FeSi_2$/p-type Si heterojunctions fabricated utilizing PLD.

2. Experimental details

NC-$FeSi_2$ thin films with a thickness of 100 nm were grown on a p-type Si(111) substrate at room temperature by means of PLD utilizing a $FeSi_2$ target. The substrate was initially removed from the oxide layer by utilizing hydrofluoric acid (HF) and then cleaned with deionized water. The cleaned substrate was instantly mounted on a substrate holder in a PLD chamber. The PLD chamber had a base pressure of 10^{-6} Torr. The distance of the substrate to the $FeSi_2$ target was fixed at 50 mm. An argon fluorine (ArF) laser beam with a wavelength of 193 nm was focus onto the rotating $FeSi_2$ target using a spherical lens. The repetition rate of the laser pulses was 10 Hz and a fulence was 10 J/cm^2. A radio frequency magnetron sputtering apparatus was used to form the back and front ohmic contacts of the heterojunctions. Pd films were formed on the back of the Si in a finger-shaped pattern, whereas Al films were formed on the whole NC-$FeSi_2$. A schematic diagram of the n-type NC-$FeSi_2$/p-type Si heterojunction fabrication utilizing PLD is shown in Fig. 1.

The crystalline structure for the NC-$FeSi_2$ thin films grown on Si substrate was characterized by utilizing X-ray diffraction (XRD; Rigaku RINT2000/PC). The measurement of the current density-voltage (*J*-*V*) curves for the heterojunctions was performed by utilizing a Keithley 2400 source meter at room temperature, in the dark and under the illumination of a 6 mW, 1.31 μm laser diode. The measurements of *C*-*V*-*f* and *G*-*V*-*f* curves were carried out with a LCR meter (Agilent E4980A) at room temperature with the *f* value range of 50 kHz - 2 MHz. From the *C*-*V*-*f* and *G*-*V*-*f* curves, the series resistance (R_s) value was computed by utilizing the Nicollian-Brews method and the N_{ss} value was computed by utilizing the Hill-Coleman method.

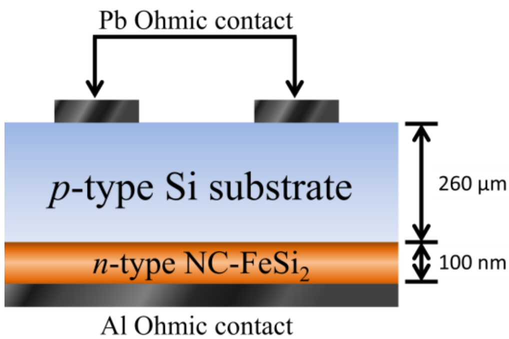

Fig. 1. Schematic diagram for n-type NC-$FeSi_2$/p-type Si heterojunctions fabricated utilizing PLD.

3. Results and discussion

Figure 2 illustrates a XRD pattern for the NC-$FeSi_2$ thin films grown utilizing PLD on a Si (111) substrate. The measurement was carried out by utilizing the grazing incidence method (2θ scan) at a fixed incidence angle of 4°. From the XRD pattern, a broad peak was observed in the 2θ range from 40-50°, it is probably attributable to the superposition from several diffraction peaks of β-$FeSi_2$. In the deposition process utilizing PLD, the nucleation of β-$FeSi_2$ instantly takes place because of the strong quenching of highly energetic particles on the surface of the Si substrate. Thus, the NC-$FeSi_2$ thin films had nuclei growth during the PLD process.

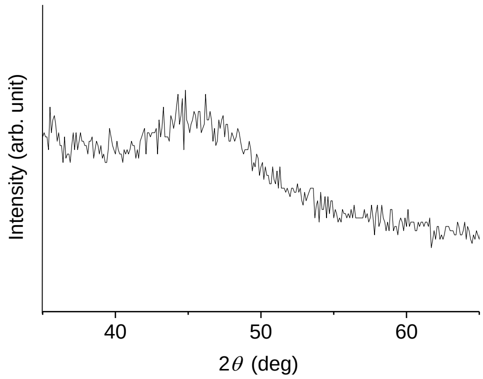

Fig. 2. XRD pattern for NC-$FeSi_2$ thin films measured utilizing a grazing incidence method (2θ scan) at a fixed incidence angle of 4°.

Figure 3 demonstrates the room temperature *J-V* curves of n-type NC-$FeSi_2$/p-type Si heterojunctions under reverse and forward bias voltage conditions, in the dark and under illumination of a 6 mW, 1.31 μm laser light. The heterojunctions demonstrated a rectifying action similar to that observed in conventional pn abrupt junctions. However, the heterojunctions demonstrated a large reverse leakage current. In addition, the illuminated current under reverse bias voltage increased slightly compared with that of dark current. These results were probably because of the existing interface states at the heterojunction interface between NC-$FeSi_2$ and Si acting as a center of leakage current and a trap center for the photo-generated carriers [14-16].

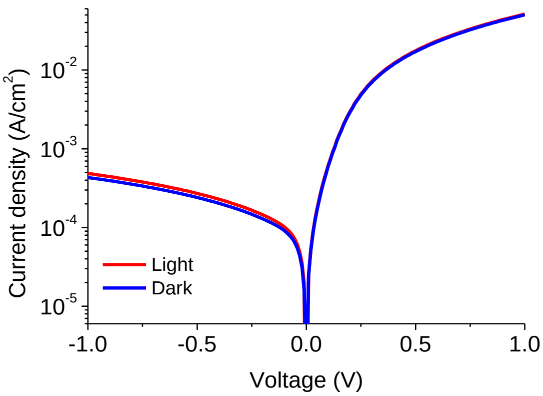

Fig. 3. The dark and illuminated *J-V* curves for n-type NC-$FeSi_2$/p-type Si heterojunctions fabricated utilizing PLD at room temperature.

The study of the dark forward *J-V* curves demonstrated the probable transportation mechanisms of the carrier via the ideality factor (n). Figure 4 shows the dark forward *J-V* curve for n-type NC-$FeSi_2$/p-type Si heterojunctions. The current increases with a V value and it shows a downward curvature at high V value. At the V value $\leq$ 0.2 V, the

J value shows a linear change with the *V* value. The utilizing the diode equation could be described as follows [20-23]:

$$J = J_0\left[\exp\left(\frac{qV}{nkT}\right) - 1\right] \quad (1)$$

where J, J_0, T, V, k, q and n are the current density, diode saturation current density, absolute temperature, applied bias voltage, Boltzmann's constant, the electron charge and ideality factor, respectively. From Eq. (1), the n value was computed from the slope of the linear part of the forward ln*J*-*V* curve through the following relationship:

$$n = \frac{q}{kT}\frac{dV}{d(\ln J)} = \frac{q}{kT}\frac{1}{slope} \quad (2)$$

Fundamentally, the predominant transportation mechanism of the carriers is a diffusion process if the n value is = 1, while the predominant transportation mechanism is a carrier recombination process if the n value is > 1 and ≤ 2. If the n value is > 2, the predominant transportation mechanism of carrier is a tunneling process.

From the computation using Eq. (2), the n value was 1.73. The implication is that the predominant transportation mechanism at the heterojunction interface between the NC-$FeSi_2$ and Si was a carrier recombination process. The existing defects in NC-$FeSi_2$ thin films might generate the deep energy levels in the bandgap. These energy levels could act as a center for recombination.

In the region of $V > 0.2$ V, the V value was sufficient to provide the carriers with sufficient energy to overcome the potential barrier at the junction. Thus, the concentration of the charge was insignificant when compared to that of the injected charges. From this, space-charge recombination takes place and controls the transportation of the carrier [24]. In essence, if the SCLC process dominates the transportation of the carrier, the J value displays a power-law dependence of the V value as follows: $J \propto V^m$. Here, the parameter m was higher than 2. The inset in Fig. 4 is a log*J*-log*V* plot for the heterojunctions. This plot shows a linear fit between log*J* and log*V* in the region of $V > 0.2$ V. The parameter m, computed from the slope of the straight line, was 2.32. The value of $m > 2$ suggests that the transportation of carrier was governed by the SCLC in this bias voltage region [25-26].

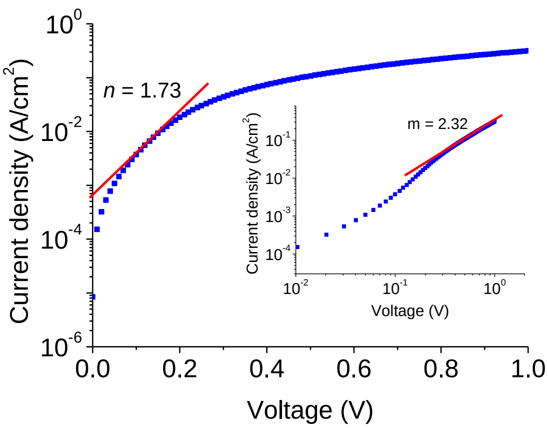

Fig. 4. Dark forward *J*-*V* curve for the n-type NC-$FeSi_2$/p-type Si heterojunctions fabricated utilizing PLD. The inset is the relationship between log*J* and log*V*.

Figure 5 (a) displays the *C*-*V*-*f* curves for the heterojunctions. The measurements performed at room temperature in the *f* value range of 50 kHz - 2 MHz showed from the curves, that the *C* value decreased when the *f* value was increased. The *G-V-f* curves for the heterojunctions are displayed in Fig. 5 (b). It was clear that the *G* value increased when the *f* value was increased.

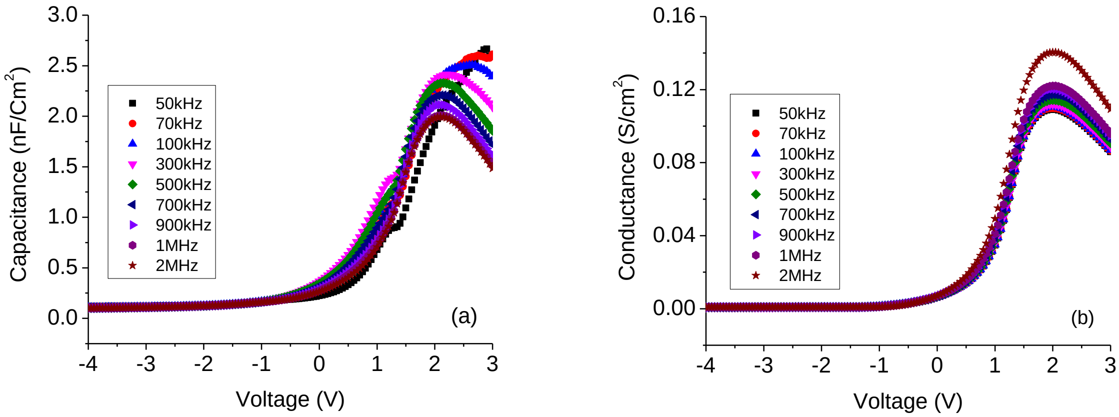

Fig. 5. (a) *C-V-f* and (b) *G-V-f* curves for the n-type NC-$FeSi_2$/p-type Si heterojunctions in the *f* values range of 50 kHz - 2 MHz.

The R_s and N_{ss} values are vital parameters for the electrical characteristics of the heterojunctions. The Nicollian-Brews method is appropriate to compute the R_s value and expressed as [27-29]:

$$R_s = \frac{G_m}{G_m^2 + (\omega C_m)^2} \quad (3)$$

Here, the G_m and C_m values are the conductance and capacitance in strong accumulation region, respectively, and ω is angular frequency.

The Hill-Coleman method was employed to compute the N_{ss} value. According to this method, the value of N_{ss} was computed from the measured *C-V-f* and *G-V-f* curves utilizing the following relationship [28-29]:

$$N_{ss} = \frac{2}{qA} \frac{(G_m/\omega)_{\max}}{\left((G_m/\omega)_{\max} C_{OX}\right)^2 + (1 - C_m/C_{OX})^2} \quad (4)$$

where $(G_m/\omega)_{max}$ and C_m are the conductance and capacitance corresponding to the maximum values, *A* is the heterojunction area, and C_{ox} is the insulator oxide layer capacitance and can be expressed as:

$$C_{OX} = C_m \left[1 + \frac{G_m^2}{(\omega C_m)^2}\right] \quad (5)$$

The R_s-*V-f* curves for the heterojunctions are displayed in Fig. 6. It was found that the R_s value decreased when the *f* value was increased. This is likely because the charges at the interface states could not follow the ac signal when the *f* value was high [27-29]. The N_{ss}-*f* curves for the heterojunctions are illustrated in Fig.7. From computation by using Eq. (4), the N_{ss} values were 2.72 x 10^{13} $cm^{-2}eV^{-1}$ at 50 kHz and 2.38 x 10^{12} $cm^{-2}eV^{-1}$ at 2 MHz. This proved the existence of interface states at the heterojunction interface between NC-$FeSi_2$ and Si. These interface states acted as the center of leakage current and trap center for photo-generated carriers and thus degraded the electrical properties of the heterojunctions. In addition, it was observed that the value of N_{ss} decreased exponentially when the *f* value was increased. In the region of the low *f* values ($\leq$ 300 kHz), the value of N_{ss} strongly depended on the *f* value, causing increasing of the *C* value in the n-type NC-$FeSi_2$/p-type Si heterojunctions. The high *C* values at low *f* values were likely owing to the excess *C* value resulting from the N_{ss}, which was in equilibrium with the semiconductor following the ac signal [30-32]. In contrast, the value of N_{ss} was almost independent of the *f* value at an *f* value > 300 kHz. Normally, the interface states are in equilibrium with the semiconductor and do not contribute to the *C* value at sufficiently high *f* values because the charge at the interface states cannot follow the ac signal [32].

Additionally, the carrier density for the grown NC-$FeSi_2$ thin films utilizing PLD is approximately 10^{19} cm^{-3}. This large carrier density value is expected to degrade the light detection of the fabricated n-type NC-$FeSi_2$/p-type Si heterojunctions due to narrowing of the depletion region that expands into the NC-$FeSi_2$ layer. Hence, the large carrier density of the grown NC-$FeSi_2$ thin films should be further suppressed.

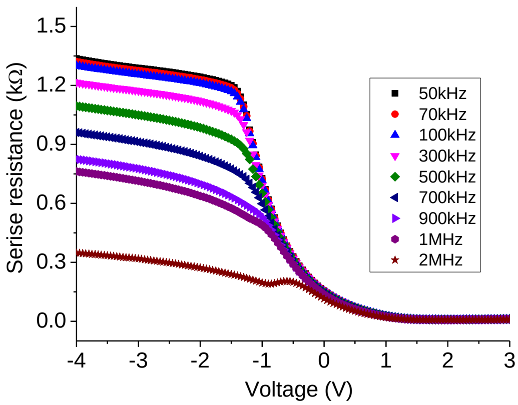

Fig. 6. R_s-*V*-*f* curves for n-type NC-$FeSi_2$/p-type Si heterojunctions fabricated utilizing PLD.

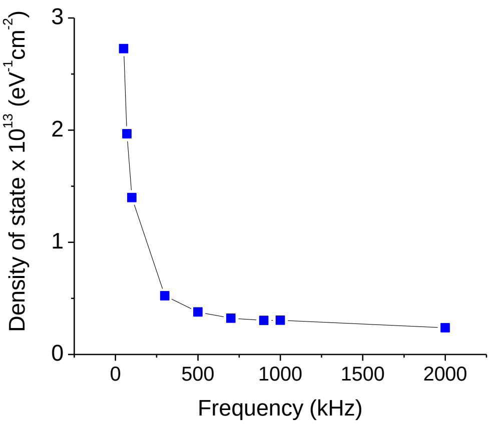

Fig. 7. N_{ss}-*f* curves for the n-type NC-$FeSi_2$/p-type Si heterojunctions fabricated utilizing PLD.

4. Conclusions

n-Type NC-$FeSi_2$/p-type Si heterojunctions were fabricated utilizing PLD at room temperature. The fabricated heterojunctions demonstrated a large reverse leakage current as well as a small NIR light response. Based on the analysis of the dark forward *J*-*V* curves, a recombination process was governed at $V \leq 0.2$ V, while a SCLC process was governed at $V > 0.2$ V. From the computation of the N_{ss} values utilizing the Hill-Coleman method, the N_{ss} values were 2.72 x 10^{13} $cm^{-2}eV^{-1}$ at 50 kHz and 2.38 x 10^{12} $cm^{-2}eV^{-1}$ at 2 MHz. This proved the existence of interface states at the heterojunction interface between NC-$FeSi_2$ and Si. These interface states acted as the center for leakage current as well as a trap center for photo-generated carriers, which was the likely cause for the degraded electrical performance of the heterojunctions at room temperature.

Acknowledgements

This work was supported financially by a research fund from AUN/SEED-Net in the Collaborative Research Program for Alumni Members (CRA) Project and King Mongkut's Institute of Technology Ladkrabang.

References

[1] T. Sunohara, K. Kobayashi, T. Suemasu, Thin Solid Films 508 (2006) 371–375.
[2] D. Leong, M. Harry, K.J. Reeson, K.P. Homewood, Nature 387 (1997) 686–688.
[3] Y. Nakamura, S. Amari, N. Naruse, Y. Mera, K. Maeda, M. Ichikawa, Cryst. Growth Des. 8 (2008) 3019–3023.
[4] N. Promros, K. Yamashita, S. Izumi, R. Iwasaki, M. Shaban, T. Yoshitake, Jpn. J. Appl. Phys. 51 (2012) 09MF02-1–09MF02-4.
[5] M. Milosavljević, L. Wong, M. Lourenço, R. Valizadeh, J. Colligon, G. Shoa, K. Homewood, Jpn. J. Appl. Phys. 49 (2010) 081401–081405.
[6] S. Izumi, M. Shaban, N. Promros, K. Nomoto, T. Yoshitake, Appl. Phys. Lett. 102 (2013) 032107-1–032107-4.
[7] H. Udono, I. Kikuma, T. Okuno, Y. Matsumoto, H. Tajima, Appl. Phys. Lett. 85 (2004) 1937–1939.
[8] J.E. Mahan, V. Le Thanh, J. Chevrier, I. Berbezier, J. Derrien, R.G. Long, J. Appl. Phys., 74 (1993) 1747–1761.
[9] J.M. Gay, P. Stocker, F. Rethore, J. Appl. Phys. 73 (1993) 8169–8178.
[10] N. Promros, R. Baba, M. Takahara, T. Mostafa, P. Sittimart, M. Shaban, T. Yoshitake, Jpn. J. Appl. Phys. 55 (2016) 06HC03-1–06HC03-4.
[11] D.N. Christensen, Phys. Rev. B 42 (1990) 7148–7153.
[12] M.C. Bost, J.E. Mahan, J. Appl. Phys. 64 (1988) 2034–2037.
[13] N. Promros, K. Yamashita, R. Iwasaki, T. Yoshitake, Jpn. J. Appl. Phys. 51 (2012) 108006-1–108006-2.
[14] N. Promros, L. Chen, T. Yoshitake, J. Nanosci. Nanotechnol. 13 (2013) 3577–3581.
[15] N. Promros, K. Yamashita, C. Li, K. Kawai, M. Shaban, T. Okajima, T. Yoshitake, Jpn. J. Appl. Phys. 51 (2012) 021301–021304.
[16] S. Funasaki, N. Promros, R. Iwasaki, M. Takahara, M. Shaban, T. Yoshitake, Phys. Status solidi C 10 (2013) 1785–1788.
[17] T. Yoshitake, M. Yatabe, M. Itakura, N. Kuwano, Y. Tomokiyo, K. Nagayama, Appl. Phys. Lett. 83 (2003) 3057–3059.
[18] M. Shaban, H. Kondo, K. Nakashima, T. Yoshitake, Jpn. J. Appl. Phys. 47 (2008) 5420–5422.
[19] K. Takarabe, H. Doi, Y. Mori, K. Fukui, Y. Shim, N. Yamamoto, T. Yoshitake, K. Nagayama, Appl. Phys. Lett. 88 (2006) 061911-1–061911-3.
[20] S. Sonmezoglu, Appl. Phys. Express 4 (2011) 104104–104106.
[21] A.A.M. Farag, I.S. Yahia, T. Wojtowicz, G. Karczewski, J. Phys. D: Appl. Phys. 43 (2010) 215102–215108.
[22] F. Ozyurt Kus, T. Serin, N. Serin, J. Optoelectron. Adv. M. 11 (2009) 1855–1859.
[23] A.A.M. Farag, I.S. Yahia, M. Fadel, Int. J. Hydrogen Energy 34 (2009) 4906–4913.
[24] M. Zhu, T. Cui, and K. Varahramyan, Microelectron. Eng. 75, (2004) 269–274.
[25] I. Hussain, M.Y. Soomro, N. Bano, O. Nur, M. Willander, J. Appl. Phys. 112 (2012) 064506-1–064506-6.
[26] L.F. Marsai, I. Martin, J. Pallares, A. Orpella, R. Alcubilla, J. Appl. Phys. 94 (2003) 2622–2626.
[27] I.S. Yahia, S. Hoda Hafez, F. Yakuphanoglu, B. Filiz Senkal M.S.A. Abdel Mottaleb, Synth. Met. 161 (2011)1299–1305.
[28] I.S. Yahai, M. Fadel, G.B. Sakr, S.S. Shenouda, F. Yakuphanoglu, J. Mater. Sci. 47 (2012) 1719–1728.
[29] Z. Ahmad, M.H. Sayyad, Kh.S. Karimov, M. Saleem Shah, Acta. Phys. Pol. A 117 (2010) 493–496.
[30] M.M. Bulbul, S. Zeyrek, Microelectron. Eng. 83 (2006) 2522–2526.
[31] S. Karatas, A. Turut, S. Altindal, Radiat. Phys. Chem. 78 (2009) 130–134.
[32] D. Korucu, A. Turut, R. Turan, S. Altindal, Mat. Sci. Semicon. Proc. 16 (2013) 344–351.